One-Forms on Meshes and Applications to 3D Mesh Parameterization

Steven J. Gortler
Computer Science Dept.
Harvard University

Craig Gotsman
Computer Science Dept.
Harvard University

Dylan Thurston
Mathematics Dept.
Harvard University

Abstract

We develop a theory of one-forms on meshes. The theory culminates in a discrete analog of the Poincare-Hopf index theorem for meshes. We apply this theorem to obtain some old and new results concerning the parameterization of 3D mesh data. Our first result is an easy proof of Tutte's celebrated "spring-embedding" theorem for planar graphs, which is widely used for parameterizing meshes with the topology of a disk by a planar tiling with a convex boundary. Our second result generalizes the first, dealing with the case where the mesh contains multiple boundaries, which are free to be non-convex. We characterize when it is still possible to achieve an injective parameterization, despite these boundaries being non-convex. The third result is an analogous Tutte-like theorem for meshes with genus 1 (topologically equivalent to the torus), paving the way for a general method to locally parameterize such meshes to the plane in a naturally seamless manner. The last result generalizes recent work of Gu and Yau. Applications of these results to the parameterization of meshes with disk and toroidal topologies are demonstrated. Extensions to higher genus meshes are discussed.

Keywords

Computer graphics, parameterization, embedding, one-form

1. Introduction

In 1963, Tutte [31] proved his celebrated "spring embedding" theorem for planar graphs. This theorem maintains that a planar graph may be easily drawn in the plane by embedding the graph boundary on a strictly convex polygon and solving a linear system for each of the two coordinates of the interior vertices. The linear system forces each interior vertex to lie at the centroid of its neighbors. Tutte proved that the result is indeed a straight line plane drawing, and, furthermore, the faces are non-degenerate, bounding convex regions in the plane.

Tutte's simple procedure remains a popular planar graph drawing method to date. It was generalized by Floater [7,8], who showed that the theorem still holds when the boundary is not strictly convex (i.e. adjacent boundary vertices may be collinear), and when each interior vertex is positioned at a general convex combination of its neighbors coordinates. The method has established itself as the method of choice for parameterizing a three-dimensional mesh with the topology of a disk to the plane in geometric modeling and computer graphics, along with a multitude of variations on this theme (e.g. [6,7,20]). The main reason for the method's popularity is that it is computationally simple, and also guarantees an injective parameterization homeomorphic to a disk, meaning that the individual planar polygons are convex and do not intersect each other. The latter is crucial for the correctness of many algorithms relying on an underlying parameterization. As such, Tutte's theorem is the basis for solutions to other computer graphics problems, such as morphing (e.g. [10,13,16]). Many recipes exist for the convex combination weights in order to achieve various effects in the parameterization. Typically, it is desirable to reflect the geometry of the original 3D mesh in the 2D parameterization, so the 2D version should be a minimally distorted 2D version of the 3D original. Depending on how distortion is measured, different weights are used. For more details, see the recent survey by Floater and Hormann [11].

Inspired by recent work on the theory of discrete vector fields [3,14,22] and their use in vector field visualization [25,30] and mesh parameterization [14], we describe a simple theory of *one-forms* on meshes. In a nutshell, this involves assigning non-zero values to the half-edges of the mesh, and analyzing the behavior of these when additional balancing conditions are imposed on the one-form. It culminates in an Index Theorem which is the discrete analog of the Poincare-Hopf index theorem for vector fields on surfaces.

One-forms on meshes turn out to be a very useful tool for mesh processing. It particular, the central result of Tutte's planar embedding theorem, when formulated in terms of the vector differences along *edges* of the graph, follows as a special case of the Index Theorem with no more than simple counting arguments and elementary geometry. The techniques used in our proof are considerably simpler than those used in proofs of different versions of Tutte's theorem which evolved over the years [2,5,8,12,26,29]. Moreover, the same arguments allow us to relax the conditions on the embedding of the mesh boundary, and even allow multiple boundaries. We show that it is sufficient that the embedding is well behaved (in a manner to be made precise later) at the vertices along the boundaries, even if they are non-convex, in order that the entire embedding be well-behaved. Since the requirement of a (pre-determined) convex boundary is the (only) major drawback of Tutte's method, this result could make Tutte's method even more popular than it already is. It introduces extra degrees of freedom into the solution, which may be use to produce less distorted parameterizations.

While variants of Tutte's theorem for meshes with the topology of a disk (namely genus 0 with at least one boundary) are easy consequences of our Index Theorem, novel and more interesting results may be obtained for meshes with higher genus. Particularly important results may be obtained for the toroidal (genus g=1) case. Since, due to the different topologies, it is impossible to map the torus homeomorphically to the plane without cutting it, the most we can hope for is a parameterization method which has this behavior *locally*. Gu and Yau [14] showed how to generate local parameterizations with so-called "conformal" structure. In the torus case, their parameterizations have the following properties: 1. Any con-

nected submesh having the topology of the disk is mapped to a disk in the plane. 2. Any two connected submeshes with non-empty intersection, all (the two submeshes and their intersection) having the topology of the disk, are mapped to disks in the plane, such that the two parameterizations coincide, up to a translation of the plane, on their intersection. Gu and Yau do not prove that the resulting mappings of the disks to the plane are free of flips. Additionally Gu and Yau restricted their attention to a very narrow subset of the possible parameterizations, to triangular meshes. We apply our one-form theory to close this gap, providing a generalization of their basic algorithm, and prove that all these parameterizations are locally injective. This may be considered a "Tutte-like" theorem for the torus.

For higher genus (g>1) meshes, the situation is more complex. Any 2D parameterization must contain $2g$-2 "double wheels", which are neighborhoods of vertices whose faces wind twice around the vertex, so the parameterization cannot be locally injective at these vertices. While we do not yet fully understand this case, we are able to provide some mathematical and algorithmic insight into how to control and generate such parameterizations.

Beyond the theoretical interest, seamless local parameterization of higher genus meshes is useful for applications such as "cut and paste" operations [4], texture mapping [18] and remeshing.

2. One-forms on Meshes and the Index Theorem

In this section we define the concept of a one-form over a mesh. This is a discrete analog of a vector field on a surface. We prove a discrete analog of the Poincare-Hopf index theorem on vector fields that relates the number of singularities in the one-form to the Euler characteristic of the mesh.

Let G=<$\mathcal{V},\mathcal{E},\mathcal{F}$> be a mesh. $\mathcal{V}$, $\mathcal{E}$ and $\mathcal{F}$ are the sets of vertices, edges and faces of G, containing V vertices, E edges and F faces respectively. In this paper we will be concerned with meshes which are closed oriented manifolds with genus g. By oriented we mean that all faces are given with consistent orientations (i.e. the two half-edges incident on two adjacent faces have opposite orientations). This induces also a consistent "orientation" (ordering) on the half-edges emanating from a vertex.

Definition 2.1: A *one-form* [G,Δz] is an assignment of a real value Δz_{uv} to each half edge e_{uv} of G such that $\Delta z_{uv} = -\Delta z_{vu}$. A one-form is called *valid* if none of the values Δz_{uv} vanish. ♦

Of particular interest are the sign patterns of a valid one-form at the half-edges associated with a vertex or face of the mesh. We use these to classify the vertices and faces, as illustrated in Figure 1. The most basic element is the *corner*, which is where the one-form changes sign (direction) as you circle a vertex or.

Definition 2.2: Let [G,Δz] be a valid one-form, v be a vertex of G and f a face of G,. The pair <v,f> is called a *corner* of [G,Δz] if $sign(\Delta z_{vu}) \neq sign(\Delta z_{vw})$, where u and w are the (unique) neighbors of v in f. In this case we say that v and f *participate* in the corner. ♦

Definition 2.3: The *index* of a vertex v in [G,Δz] is $ind(v) = (2-corn(v))/2$, where $corn(v)$ is the number of corners of [G,Δz] in which v participates. A vertex v of G is called a *non-singular* vertex of [G,Δz] if $ind(v)=0$ and a *saddle* vertex if $ind(v)<0$. If $ind(v)=1$, and all values of Δz at v are positive, v is called a *source*, otherwise it is called a *sink*. ♦

Definition 2.4: The *index* of a face f in [G,Δz] is $ind(f) = (2-noncorn(f))/2$, where $noncorn(f)$ is the number of non-corners of [G,Δz] in which f participates. A face f of G is called a *non-singular* face of [G,Δz] if $ind(f)=0$ and a *saddle* face if $ind(f)<0$. If $ind(f)=1$, it is called a *vortex*. ♦

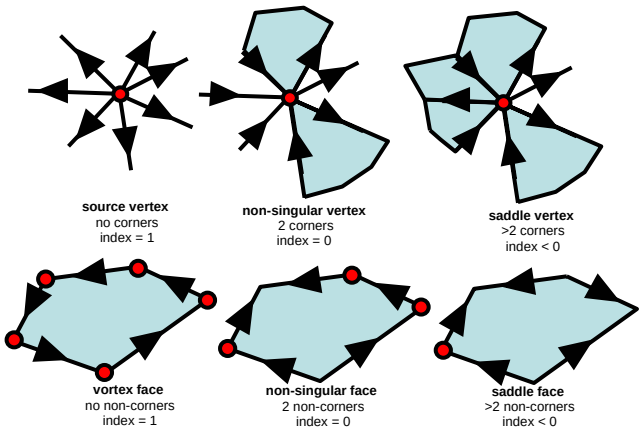

Figure 1: Illustration of Definitions 2.2-2.4. Classification of vertices by number of corners and faces by number of non-corners. Arrows denote the orientation of the half-edge with a positive value of the one-form. A red vertex in a blue face is a corner.

Note that since (by definition) the number of corners at a vertex and the number of non-corners in a face must be even, the index is always an integer. Moreover, the index can never exceed +1. When the index is negative, its magnitude indicates the frequency of the one-form sign changes on its half-edges. The following theorem now characterizes the global distribution of indices of vertices and faces of a mesh in terms of its genus:

Theorem 2.5 (Index Theorem): If G is a closed oriented manifold mesh of genus *g,* then any valid one-form [G,Δ*z*] satisfies

$$\sum_{v\in\mathcal{V}} ind(v) + \sum_{f\in\mathcal{F}} ind(f) = 2-2g$$

Proof:

$$\begin{aligned}
&\sum_{v\in\mathcal{V}} ind(v) + \sum_{f\in\mathcal{F}} ind(f) \\
&= \tfrac{1}{2}\sum_{v\in\mathcal{V}} (2-corn(v)) + \tfrac{1}{2}\sum_{f\in\mathcal{F}} (2-noncorn(f)) \\
&= V+F-\tfrac{1}{2}\left(\sum_{v\in\mathcal{V}} corn(v) + \sum_{f\in\mathcal{F}} noncorn(f)\right) \\
&= V+F-\tfrac{1}{2}\left(\sum_{v\in\mathcal{V}} corn(v) + \sum_{f\in\mathcal{F}} ((valence(f)-corn(f))\right) \\
&= V+F-\tfrac{1}{2}\left(\sum_{v\in\mathcal{V}} corn(v) + \sum_{f\in\mathcal{F}} valence(f) - \sum_{f\in\mathcal{F}} corn(f)\right) \\
&= V+F-\tfrac{1}{2}\left(\sum_{f\in\mathcal{F}} valence(f)\right) \\
&= V+F-E \\
&= 2-2g
\end{aligned}$$

The fifth equality is due to the total number of corners in the mesh being the same whether one counts over each vertex or over each face. The sixth equality is due to the fact that each edge appears in the valence count of two faces. The seventh equality is Euler's formula. ♦

A special case of our Index Theorem was obtained by Banchoff [1] and Lazarus and Verroust [19]. However, their theorem applies only to so-called *null-cohomologous* one-forms (arising from the differences of a scalar potential field defined on the mesh vertices) over a triangle mesh, and thus does not consider faces of non-zero index. Thus their summation of indices is over vertices exclusively, whereas we sum over faces as well. Indeed, in Section 3, we deal with non-triangular interior faces (which we need to prove are not saddles), and more importantly, with a non-convex exterior face (that in fact *is* a saddle).

As we will see, we will be able to characterize the scenario of Tutte's theorem in terms of valid one-forms on a genus-0 mesh. These one-forms will have certain balances, which will constrain the types of non-singular faces and vertices that can occur. We now restrict our attention to this subset of one-forms.

Definition 2.6: Given a set of (not necessarily symmetric) positive weights u_{ij} associated with each half edge in G and a one-form [G,Δz], we call a face *f, closed wrt* (*with respect to*) *u* if

$$\sum_{h \in \partial f} u_h \Delta z_h = 0 \tag{1}$$

∂f is the *boundary* operator applied to the face, yielding the set of half-edges incident on the face, ordered by the face orientation. ♦

Definition 2.7: Given a set of (not necessarily symmetric) positive weights w_{ij} associated with each half edge in G and a one-form [G,Δz], a vertex is called *co-closed wrt w* if

$$\sum_{h \in \delta v} w_h \Delta z_h = 0 \tag{2}$$

where δv is the *coboundary* operator applied to the vertex, yielding the set of half-edges incident on the vertex, ordered by the vertex orientation. ♦

One-forms which everywhere satisfy (1) and (2) are called *harmonic* one-forms. Closedness of faces and co-closedness of vertices are related to their indices:

Corollary 2.8: If a face *f* is closed in a valid one-form wrt to some set of positive weights, then $ind(f) \leq 0$. If a vertex *v* is co-closed wrt to some set of positive weights, then $ind(v) \leq 0$.

Proof: If *f* were a vortex, then all of the terms in (1) would be positive and thus could not sum to zero. The same holds for *v* a source or sink. ♦

3. Parameterizing a Disk

Tutte's theorem may be stated as follows:

Theorem 3.1 (Tutte [31]): Let G=<$\mathcal{V},\mathcal{E},\mathcal{F}$> be a 3-connected planar graph with boundary vertices $\mathcal{B} \subset \mathcal{V}$ defining a unique infinite exterior face f_e. Suppose ∂f_e is embedded in the plane as a (not necessarily strictly) convex planar polygon, and each interior vertex is positioned in the plane as a convex combination of its neighbors, then the straight-line drawing of G with these vertex positions is an embedding (no edges cross). In addition, this embedding has strictly convex interior faces. ♦

Such an embedding is found by solving the following linear system for the x and y coordinate values of the vertices:

$$\begin{aligned} \sum_{v_j \in N(v_i)} w_{ij} x_j &= x_i \qquad i = 1,..,V-B \\ \sum_{v_j \in N(v_i)} w_{ij} y_j &= y_i \qquad i = 1,..,V-B \\ x_i &= b_i^x \qquad i = V-B+1,..,V \\ y_i &= b_i^y \qquad i = V-B+1,..,V \end{aligned} \tag{3}$$

where we label the interior vertices with $\{1,..,V\text{-}B\}$, and the remaining boundary vertices with $\{V\text{-}B+1,..V\}$. The w_{ij} are any set of positive numbers with unit row sums (hence the term *convex combinations*). We do not assume that w_{ij} are symmetric. $N(v_i)$ is the set of vertices neighboring v_i.

3.1 Single Convex Boundary

In Tutte's scenario, the boundary polygon, described by $[b^x,b^y]$ is assumed to be (not necessarily strictly) convex. It is well known that (3) has a unique solution $[x,y]$, which we call a *Tutte solution* for G. This follows directly from the fact that the linear system is irreducible, and is weakly diagonally dominant with at least one strongly diagonally dominant row [32]. We denote by $[G,x,y]$ the straight line drawing of this solution.

Proving Tutte's theorem amounts to showing that $[G,x,y]$ is a straight-line planar embedding (ie. the mapping to the plane is injective). We proceed in this direction by examining the properties of $span(x,y)$ – all the different projections of the drawing, and constructing a one-form on G. For any choice of reals α and β, define $z \equiv \alpha x + \beta y$. At every interior vertex v_i, define:

$$\begin{aligned} z_i &\equiv \alpha x_i + \beta y_i \\ &= \alpha \sum_{v_j \in N(v_i)} w_{ij} x_j + \beta \sum_{v_j \in N(v_i)} w_{ij} y_j \\ &= \sum_{v_j \in N(v_i)} w_{ij} (\alpha x_j + \beta y_j) \\ &= \sum_{v_j \in N(v_i)} w_{ij} z_j \end{aligned} \tag{4}$$

and at the boundary vertices:

$$z_i \equiv \alpha b^x{}_i + \beta b^y{}_i$$

Now define the one-form $\Delta z_{ij} = -\Delta z_{ji} \equiv z_j - z_i$. Since the rows sum to unity, (4) implies that every interior vertex v of $[G,\Delta z]$ is co-closed wrt w:

$$\sum_{h \in \delta v} w_h \Delta z_h = 0$$

Furthermore, because the Δz are differences of the z values at vertices, they must sum to zero along any directed closed loop in G. In particular, each face f satisfies

$$\sum_{h \in \partial f} \Delta z_h = 0$$

meaning Δz is closed wrt unit weights.

Figure 2 illustrates the generic structure of the one-form Δz. Due to the convexity of the boundary $\mathcal{B}$, a property which is preserved under linear transformations, $\mathcal{B}$ will generically contain one vertex with a maximum z and one with a minimum z. Every other vertex of $\mathcal{B}$ has one neighbor in $\mathcal{B}$ with a strictly

greater z value, and its other neighbor in $\mathcal{B}$ with a strictly smaller z value. As a result, none of these vertices can be sources or sinks in $[G,\Delta z]$, i.e. they must have non-positive index.

The following lemma concerning one-forms closely corresponds to the scenario of the Tutte embedding theorem.

Lemma 3.2: If G has genus 0, $[G,\Delta z]$ is a valid one-form such that all F faces are closed wrt some set of positive weights, V-B vertices are co-closed wrt some set of positive weights and of the remaining B vertices, B-2 have index ≤ 0, then $[G,\Delta z]$ has no saddle vertices and no saddle faces.

Proof: By the Index Theorem (Theorem 2.5), the sum of the indices over all of the faces and vertices on a spherical mesh must total +2. Due the assumption, all the faces and V-2 vertices can contribute only non-positive values to this sum. The only way to achieve the sum of +2 is for all F faces and V-2 of the vertices to have vanishing index, and for the remaining two vertices to have the maximal index value of +1. In other words, $[G,\Delta z]$ has no saddles (but it does have a source vertex and a sink vertex). ♦

It is possible for a one-form, Δz as constructed above from $[G,x,y]$, to vanish on interior or boundary edges. This one-from will be invalid and Lemma 3.2 will not directly apply. Fortunately it is possible to slightly perturb any such a one-form into a valid one-form without changing the signs of the one-form values along the half-edges that have non-zero values. Appendix A shows how this is achieved. The resulting valid one-form will now have vertices that are not co-closed. But the important property of the vertices (resp. faces) in the proof of Lemma 3.2 is not their co-closedness (resp. closedness), but rather the weaker property that they are *mixed* - have both positive and negative values of the one-form on the half-edges emanating from them in δv (resp. half-edges circling ∂f) and are thus guaranteed to have non-positive index.

This, and Lemma 3.2 combined with Corollary 2.8, immediately imply:

Corollary 3.3: If $[G,x,y]$ is a Tutte solution, then for any α, β and $[G,\Delta z]$ constructed as in (4) (and perturbed if necessary as described in Appendix A), no vertex or interior face is a saddle in $[G,\Delta z]$. ♦

Finally, we need to show that if the drawing $[G,x,y]$ does not have the required properties, then there must be a $z \in span(x,y)$ such that $[G,\Delta z]$ has either a saddle vertex or a saddle face. The required properties of $[G,x,y]$ that will make it a planar embedding are that all faces are simple, convex, and disjoint. The next set of definitions will formalize this. However, to proceed, we rely on the fact that there are no degeneracies in a Tutte solution. The following Lemma is proved in Appendix B, and we proceed under this assumption.

Lemma B.5: In a Tutte solution there can be no face with zero area, no edge of zero length and no angle of 0 or π within any interior face. ♦

Definition 3.4: A face f of G is called a *convex* face of $[G,x,y]$ if its boundary is a simple strictly convex polygon in the plane. ♦

Definition 3.5: Consider the angles α_i formed between the edges emanating from a vertex v in $[G,x,y]$, as ordered by the graph topology. v is called a *wheel* vertex of $[G,x,y]$ if $0<\alpha_i<\pi$ and $\Sigma\alpha_i=2\pi$. ♦

Figure 3 shows some examples of non-convex faces and vertices which are not wheels.

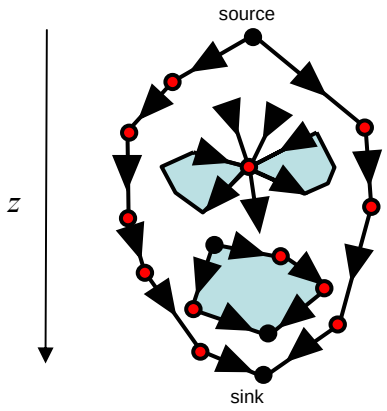

Figure 2: The generic structure of a Tutte solution, looking at the one-form which is the projection of the drawing along the vertical *z*. All vertices and faces are non-singular, except for one source and one sink on the boundary. Arrows mark the orientation of the half-edges possessing positive values of the one-form.A red vertex in a blue face is a corner.

Theorem 3.6: If [G,*x,y*] is a Tutte solution, then all interior faces of G are convex and all interior vertices are wheels.

Proof: Suppose the face *f* of G is non-convex in [G,*x,y*]. Then there exists a line *l* in the plane that intersects more than two edges of *f*. Rotate the plane using a matrix $\begin{pmatrix} \beta & -\alpha \\ \alpha & \beta \end{pmatrix}$ such that *l* is horizontal (see the dashed lines in Figure 3). The vector $z = \alpha x + \beta y$ represents the vertical component of the rotated drawing. In the resulting [G,Δz], there must be vertices which are not corners between the edges of *f* that *l* intersects. This means that the half-edges circling ∂f exhibit at least two sign changes (ignoring zero values). If Δz is valid, then *f* is a saddle face in [G,Δ*z*]. (If Δz is invalid, then by Lemma A.5, after it is perturbed *f* is a saddle face in [G,Δ*z*]). This contradicts Corollary 3.3.

Likewise, suppose a vertex *v* of G is not a wheel, then there exists a line *l* through *v* in the plane that intersects more than two wedges of *v*. An identical argument shows that with the appropriate choice of α and β, *v* becomes a saddle in [G,Δ*z*], again contradicting Corollary 3.3. ♦

As a result of Theorem 3.6, the one-ring of faces around each interior vertex maps homeomorphically to a disk in the plane. (Similar reasoning shows that the "half-ring" of interior faces around each boundary vertex maps homeomorphically to a "half-disk"). In other words, any two adjacent faces in the drawing are disjoint. This is what Floater [7] calls *local injectivity*. The following theorem establishes also *global* injectivity, namely that *any* two faces in the drawing are disjoint.

Theorem 3.7: All of the faces in a Tutte solution are disjoint.

Proof: Each face is strictly convex in the plane, so has a well-defined orientation. By Theorem 3.6, the one-ring of faces around each vertex is embedded as a disk, so all of these orientations are identical. Each point in the plane is contained in a finite number of the convex faces – its *face count*. Imagine moving that point over the plane and tracking this face count. Because the face orientations are all identical, the face count does not change when the point crosses over an interior edge. The boundary is convex, hence simple. Hence the face count changes by 1 when passing over a boundary edge, and is 0 outside the boundary. It follows that the face count must be equal to 1 everywhere on the interior. ♦

This concludes our proof of Tutte's theorem.

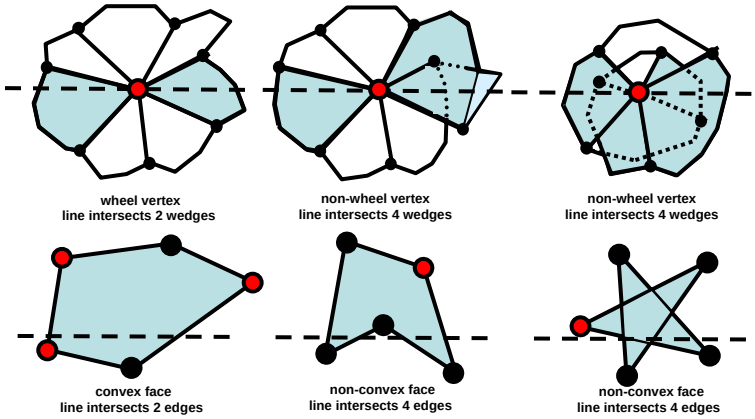

Figure 3: Illustration of Definitions 3.4 and 3.5 and proof of Theorem 3.6. The horizontal dashed lines show that there always exists a line that intersects a non-wheel in more than two wedges and a non-convex face in more than two edges. A red vertex paired with a blue face indicates a corner in the one-form which is the projection along the vertical.

3.2 Multiple Non-Convex Boundaries

While the scenario of Tutte's theorem requires the single boundary to be convex in order that the resulting drawing be a planar embedding (i.e. contain only wheel vertices and convex faces), our theory permits the presence of non-convex vertices (so-called *reflex* vertices) in the boundary. In fact, we permit the presence of *multiple* non-convex boundaries.

We can thus think of our mesh G as a topological sphere with some faces labeled as *exterior*. One of these exterior faces will be *infinite* in the planar drawing, while the rest will be *finite*. The boundaries of these exterior faces will be mapped to the plane, and impose boundary conditions in the system of equations (3). In order to produce a correctly oriented drawing, we will require that the turning number of the boundary of the infinite exterior face be $+2\pi$ and the turning number of the boundaries of the finite exterior faces be -2π. We will also require that the reflex vertices be wheels. As we will see, these restrictions force the rest of the drawing to behave as well. First a few definitions:

Definition 3.8: Let P be a straight line mapping of an oriented polygon to the plane, with all edges having positive length (but allowed to cross). The *turning angle* of P at vertex v is the external angle at v as one traverses P consistent with its orientation. This angle is positive if the turn at v is a right turn in the plane and negative if the turn is a left turn. The *turning number* of P is the sum of the turning angles at the vertices of P. ♦

Definition 3.9: Let P be as above. A vertex v is called *convex* in P if the turning angle at v is non-negative. Otherwise v is called *reflex* in P. ♦

Definition 3.10: Let P be as above. A vertex v of P is called *extremum* relative to a direction d in the plane, if the edges emanating from v all project positively onto d. ♦

Lemma 3.11: Let P be as above with turning number $+2\pi$ (-2π resp.). Denote by C its set of convex extrema, and by R its set of reflex extrema with respect to any direction d. Then $|C|-|R|=2$ ($|R|-|C|=2$ resp.).

Proof: Imagine "flattening" the polygon along direction d. Then, at the (flat) limit, the turning angle is $+\pi$ at each $v \in C$, $-\pi$ at every $v \in R$, and 0 at all other vertices. Since the total turning number is $+2\pi$ (-2π resp.), this means that $\pi(|C|-|R|) = 2\pi$ ($\pi(|C|-|R|) = -2\pi$ resp.), namely $|C|-|R|=2$ ($|R|-|C|=2$ resp.). ♦

In our parameterization setting, the boundary of each exterior face is mapped to the plane. This mapping imposes boundary conditions on the linear system of equations (3). Under this mapping (and chosen orientation for G), the turning number of each external face's boundary is well-defined, and its vertices may be characterized as convex or reflex.

Lemma 3.12: Suppose that: 1) G is an oriented 3-connected mesh of genus 0 having multiple exterior faces. 2) The boundary of the infinite exterior face is mapped to the plane with positive edge lengths and turning number 2π. 3) The boundaries of the finite exterior faces are mapped to the plane with positive edge lengths and turning number -2π. 4) $[G,x,y]$ is the straight line drawing of G where each internal vertex is positioned as a convex combination of its neighbors. 5) In $[G,x,y]$ the reflex vertices of all of the exterior face boundaries are wheels. Then for any α, β and $[G,\Delta z]$ constructed as in (4), no vertex or interior face is a saddle in $[G,\Delta z]$.

Proof: As illustrated in Figure 4, assume the N boundaries of $[G,x,y]$ form one infinite and N-1 finite polygonal exterior faces in the plane with B_i vertices each, of which C_i are convex vertices, and R_i are reflex vertices. Consider the one-form $[G,\Delta z]$. Since the extrema vertices of the exterior faces are all non-corners in those faces, the indices of the exterior faces are $1-(C_i+R_i)/2$. The interior faces are closed and the interior vertices are co-closed, hence their indices are ≤ 0. Having both positive and negative values of Δz on their co-boundaries, the indices of the non-extremal boundary vertices are ≤ 0. Being wheels, the indices of the reflex extrema are also ≤ 0. Trivially, the convex extrema have indices ≤ 1. Denote by s the sum of the (negative) indices of the saddle interior faces and vertices. So the sum of the indices over the entire mesh is $\leq \Sigma(1-(C_i+R_i)/2)+ \Sigma C_i+s$. But the Index Theorem maintains that this sum is +2, implying $2 \leq N+\Sigma(C_i-R_i)/2+s$. Now Lemma 3.11 implies that $\Sigma(C_i-R_i) = 2-2(N-1) = 4-2N$. This means that $s \geq 0$, but since, by definition $s \leq 0$, we conclude that $s = 0$, namely, saddles do not exist in the interior faces or vertices. ♦

Using arguments identical to those of the previous section, we conclude:

Theorem 3.13: Under the conditions of Lemma 3.12, all interior faces of $[G,x,y]$ are convex and all vertices are wheels. Moreover, if all the exterior faces are embedded as disjoint *simple* polygons (edge crossings are not allowed), then all faces of $[G,x,y]$ are disjoint. ♦

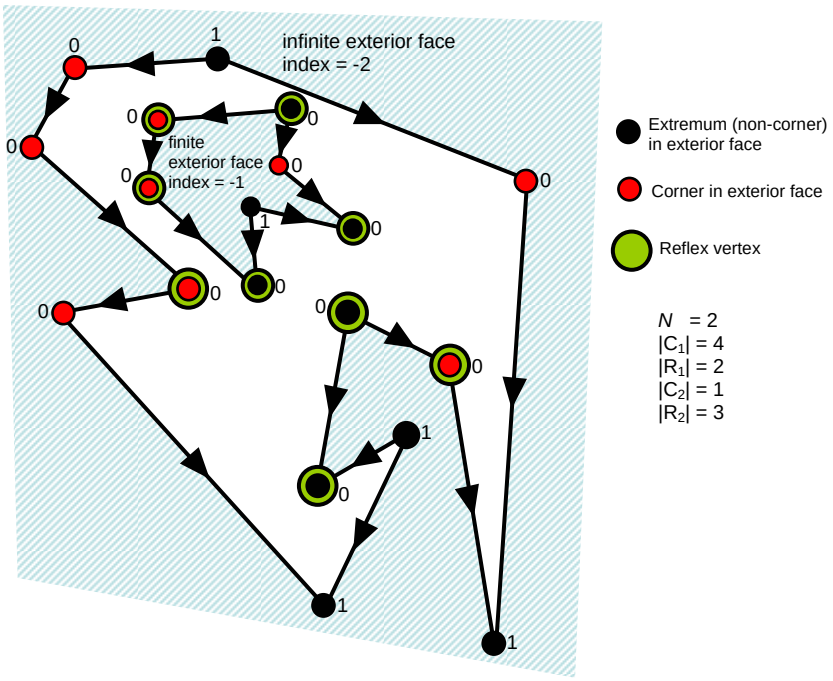

Figure 4: The multiple non-convex boundary scenario. The one-form considered is the projection on the vertical. Arrows mark the half-edges having positive values of the one-form. Vertices are labeled with their indices.

A natural question is whether Theorem 3.13 is of any use in practical parameterization scenarios, as Tutte's theorem is. Forcing the boundary vertices to form a convex shape, as in the Tutte scenario, is easy, but is it possible to relax that requirement, yet force these vertices to be wheels without compromising the co-closedness of neighboring vertices ? One way to do this is to replace the $2B$ linear boundary equalities in (3) with B_F *bilinear inequalities*, where B_F is the number of interior faces along the boundaries, expressing the fact that all the wedges formed by these faces have the correct orientation. This involves considerably less inequalities than what would have been required had Theorem 3.13 not been true, as in that case, at least F inequalities would have been required, one for each face, in order to guarantee an injective embedding. However, being inequalities (as opposed to equalities), this will introduce many degrees of freedom into the solution.

A more concrete approach is to require more of the boundary. In many applications, a *conformal* parameterization is sought, meaning one that preserves angles as much as possible in the transition from 3D to 2D. Traditional linear conformal parameterizations use the Tutte method with *cotangent* weights [24], however, these weights can sometimes be negative, hence are actually inappropriate for the Tutte scenario. Floater [9] recently proposed to replace these cotangent weights with so-called *mean-value* weights, which are always positive and seem to result in parameterizations which are close to conformal. The Angle-Based Flattening (ABF) method of Sheffer and de Sturler [26] addresses the problem in the triangular case by solving directly for the angles of the triangles, and reconstructing the embedding from that. Forcing all the angles to assume values in the interval $[0,\pi]$ (along with other constraints) guarantees that the resulting 2D triangulation is injective. This approach is non-linear, but has the advantage of a free boundary.

We propose an alternative method to those described above, taking advantage of Theorem 3.13 to solve the conformal mapping problem, stated more precisely as follows: Given a 3D triangle mesh M as input, with angles α_i incident on the boundaries, and β_i elsewhere, construct an injective 2D parameterization of M, such that the 2D angles are as close as possible to α_i and β_i. Theorem 3.13 implies that in order to ob-

tain an injective 2D embedding, it suffices to force the boundary angles to be positive and close to α_i, and compute the interior vertices' positions by solving a linear system using mean-value weights derived from the β_i. Since α_i will typically be very positive (meaning sufficiently distant from zero), this will force the 2D boundary angles to be positive, hence the boundary vertices will be wheels, and the result an injective embedding. Since we do not know in advance which vertices will be reflex, we force *all* boundary vertices to be wheels.

Figure 5 shows some results of this parameterization algorithm on two 3D input meshes. The first input is the "ear" mesh, which is embedded as a triangulation with a non-convex boundary. Note how the 2D boundary has a shape very close to that of the 3D boundary and how the angles are very similar. The second input is the "face" mesh, containing multiple boundaries ("holes"). Note that the hole corresponding to the "mouth" has a non-convex character in the 3D input, which is preserved in the resulting 2D embedding. The third input is a hemisphere, in which three slits have been cut. The resulting 2D embedding takes advantage of these slits when forming the boundary for the resulting conformal parameterization.

It is not clear at this point whether it is possible to satisfy the conditions of Theorem 3.13 with $2B$ more complicated, yet still linear, equations involving the boundary vertices, possibly coupling the x and y coordinates (which the other balance equations do not attempt to do). An example of such equations was demonstrated by Desbrun et al [5], also attempting parameterization of a disk-like mesh with free boundary. It is not clear whether those equations actually force the boundary vertices to be wheels, hence it is not obvious that the result is guaranteed to be an injective embedding.

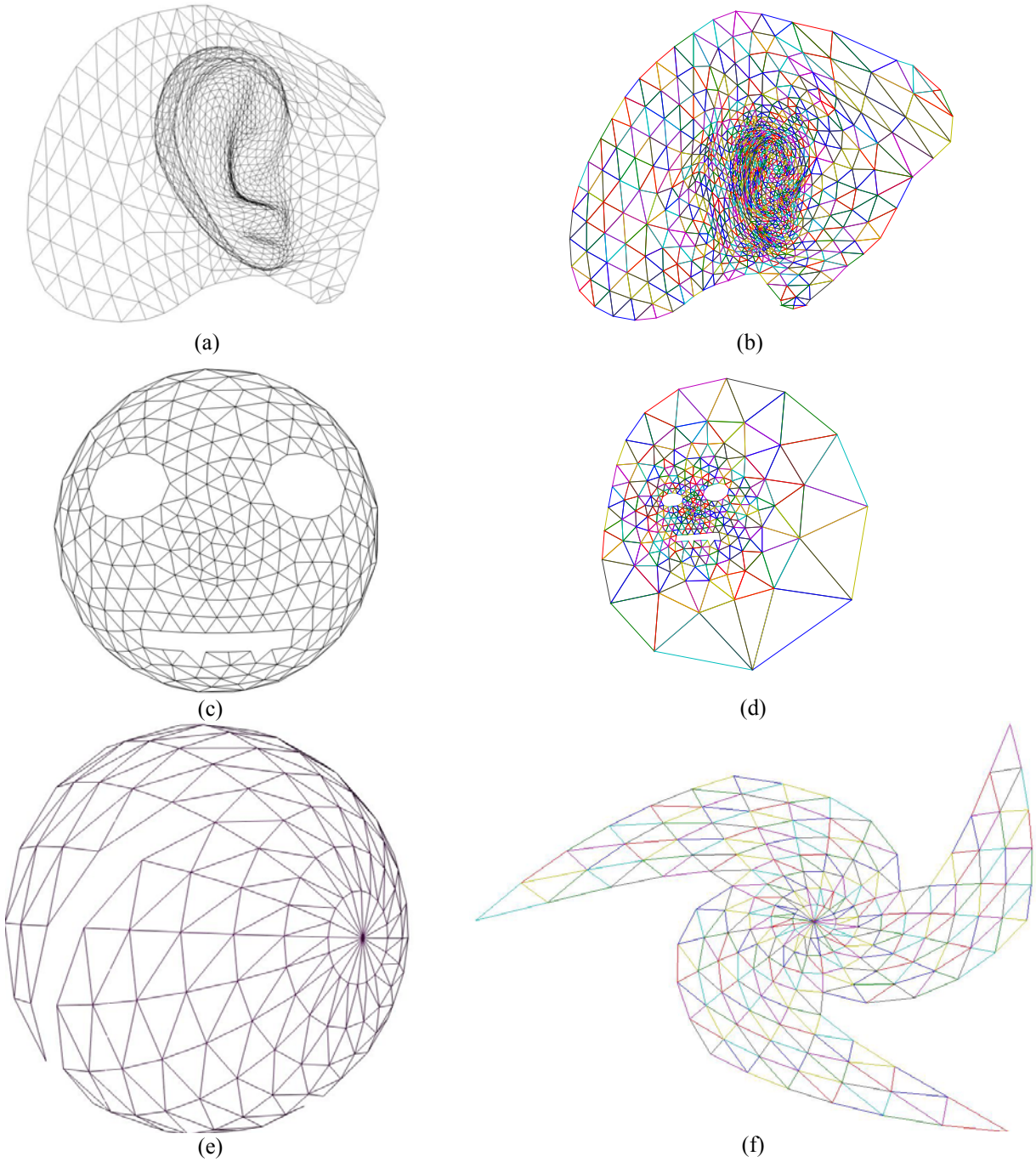

Figure 5: Parameterizing a mesh with free boundaries: **(a),(c)**,**(e)** Original 3D meshes. **(b),(d),(f)** 2D parameterizations of (a), (c) and (e) when boundaries (finite and infinite) are free but forced to have wheel vertices whose 2D angles are as close as possible to 3D originals. Mean-value weights were used in for the interior vertices.

4. Parameterizing a Torus

While our theory of one-forms on meshes allowed us to obtain Tutte's theorem for disks and extensions, it has a more natural application in the case of a toroidal mesh. This case is actually easier to analyze because, in its simplest form, there is no boundary to complicate matters. On the other hand, it is more difficult to envision a parameterization in this case, since the torus obviously cannot be mapped in an injective manner to the plane. The traditional solution to this is to cut the mesh along an artificial boundary to form a disk, and then parameterize as any other disk-like mesh. While this is certainly possible, cutting the mesh introduces new problems such as optimization of this boundary, and obvious discontinuities in the parameterization along the boundary.

Another way to parameterize a toroidal mesh without encountering the cutting problem, is to parameterize it *locally*, meaning injectively embed any submesh with disk topology, yet in a way such that all local parameterizations fit together in a seamless manner. So, while we never attempt to parameterize the entire mesh, if two intersecting disk-like regions (whose intersection is also disk-like) are parameterized to the plane, the parameterization should coincide on the intersection, possibly after an appropriate translation. See Figure 6. One-form theory provides a way of doing this seamless local parameterization by working with a pair of one-forms. Each one-form provides the information needed to synthesize one of the coordinate values at the vertices in the plane. As in the case of the disk, we will see that the key is to use two saddle-free harmonic one-forms.

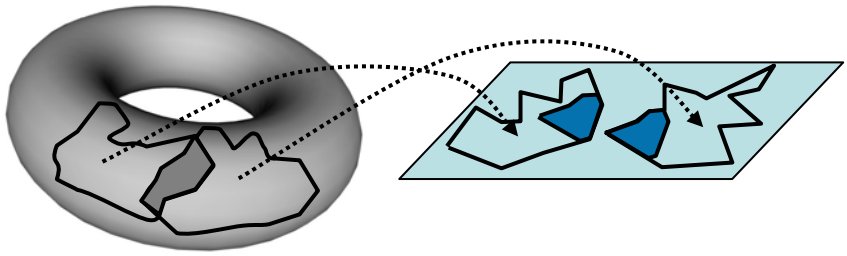

Figure 6: Seamless local parameterization of disk-like submeshes of the torus.

Seamless local parameterization is important for a variety of mesh processing applications, in particular "cutting and pasting" between meshes, as described by Biermann et al [4], texture mapping and remeshing.

The basic method for seamless local parameterization was first introduced by Gu and Yau [14], using the same one-form concept, but they did not analyze whether this method would in fact produce a proper embedding. Here, we prove, based on the Index Theorem (Theorem 2.5) that this is indeed the case. In this sense, this is a Tutte-like theorem for the torus.

Our theorem applies to a more general case than that originally explored in [14]. Gu and Yau dealt specifically, with special *conformal* weights in their equation (1), only dealt with pairs of one-forms related by the so-called Hodge star operator, and only considered meshes with triangular faces. Our theorem applies to *arbitrary* positive weights, *any* pair of linearly independent harmonic one-forms, and applies meshes with *arbitrary* sized faces.

A recent paper of Steiner and Fischer [28] makes observations similar to ours, in particular that linearly independent harmonic one-forms generate locally-injective parameterizations of the torus. The proofs they give, however, are rather complicated.

As opposed to the disk case, where we considered the planar coordinates of the embedding, and then converted them to a one-form to prove Tutte's theorem, in the toroidal case we start off with a one-form, and then synthesize the local embeddings from that. We begin with a general theorem concerning one-forms on higher genus meshes. This theorem is proven in [3,14,22], where it is considered a discrete analog to the Hodge decomposition theorem for vector fields on surfaces. The related fact that any harmonic vector field on a surface can be expressed as the sum of a rotation-free field and a divergence-free field is the basis of the vector visualization techniques of Polthier and Preuss [25] and Tong et al. [30].

Theorem 4.1 [3,14,22]: If G is a closed oriented manifold mesh of genus *g,* then the linear space of harmonic one-forms wrt some set of positive weights has dimension 2*g*. ♦

The reader may be convinced of the correctness of Theorem 4.1 by observing the following: The rank of the set of equations (1) is *F*-1. This is despite the fact that there are *F* equations, since if all but one of the faces are closed, then this implies that the last face must be closed too. The same is true for the set of equations (2) – their rank is *V*-1. The number of unknowns is *E*, hence the dimension of the solution space is *E*-(*V*+*F*-2), which, by Euler's formula, is 2*g*.

Note that Theorem 4.1 implies that the only harmonic one-form on a closed spherical mesh is the degenerate (all zeros) one-form. Luckily this is not the case for the disk, due to the existence of non-harmonic vertices along the boundary, facilitating Theorems 3.6 and 3.13.

Theorem 4.1 implies that the space of harmonic one-forms on the torus is two-dimensional. Two linearly independent one-forms may be sampled from this space in a variety of ways. Note that the closedness of the one-form implies that the sum of the one-form on any edge loop enclosing a disk-like submesh will vanish. However, the analogous sum on any loop *circling* the handle of the torus will generally not vanish. Gu and Yau organized the space of harmonic one-forms by specifying the sums of the one-form (the "signatures") around loops that form a basis for the first homology group of G.

The following is an analog of Lemma 3.2 for a torus:

Lemma 4.2: If G is a closed manifold mesh with genus 1 and Δz a valid harmonic one-form on G*,* then [G,Δz] has only non-singular vertices and faces.

Proof: By Theorem 2.5, the sum of the indices of the vertices and faces of [G,Δz] is 0. Since all vertices are co-closed and all faces are closed, their indices are all non-positive. Thus the only way these indices can sum to zero is if they are all zero. ♦

To construct a local parameterization for the torus, we choose any two linearly independent harmonic one-forms, Δx and Δy, which are linearly independent solutions to (1) and (2) with unit weights in (1). Now, given a submesh with the topology of a disk, assign the coordinates (0,0) in the planar parametric domain to an arbitrary vertex v_0 of that submesh. Any other vertex is assigned coordinates by *integrating* (summing) the one-form along a directed path from v_0 to *v.* Since the one-form is closed, it does not matter which path is used:

$$\begin{aligned}(x_0, y_0) &= (0,0)\\ (x_i, y_i) &= \left(\sum_{h \in P(v_0, v_i)} \Delta x_h, \sum_{h \in P(v_0, v_i)} \Delta y_h \right)\end{aligned} \tag{5}$$

Because the space is two-dimensional, it does not really matter which two harmonic one-forms are used, as long as they are independent. Any other pair of one-forms will be a linear combination of these, meaning the resulting parameterizations will be related to each other by an affine transformation.

We now use Lemma 4.2 to prove the analog of Theorem 3.6 for the torus:

Theorem 4.3: If G is a 3-connected manifold mesh with genus 1, Δx and Δy two non-degenerate and linearly independent harmonic one-forms on G, and G' a submesh of G with the topology of a disk, then all faces of [G',*x*,*y*] are convex and all vertices of [G',*x*,*y*] are wheels, where *x* and *y* are constructed as in (5).

Proof: Identical to the proof of Theorem 3.6, using Lemma 4.2 instead of Lemma 3.2. ♦

Note that if the method of (5) is run twice, each time with a different vertex as v_0, the two resulting parameterizations will, by definition, be related to each other by a simple translation in the plane. The translation vector will be the coordinates of the second origin in the first parameterization (or vice versa).

Theorem 4.3 is a statement of local injectivity. It can also be shown that a pair of harmonic one-forms, in fact creates a globally injective mapping from the universal cover of the torus to the entire plane. As a result, there can be no edge crossings in these parameterizations. The proof relies on Theorem 4.3, but also on some notions from algebraic topology, and is thus omitted.

Figure 7 shows such an parameterization of a toroidal mesh, where the disk-like submesh is actually the entire mesh, after it was cut twice along two *basis* loops of the handle. Because of the periodicity of the torus, the resulting embedding can be used to tile the plane in a doubly-periodic seamless manner.

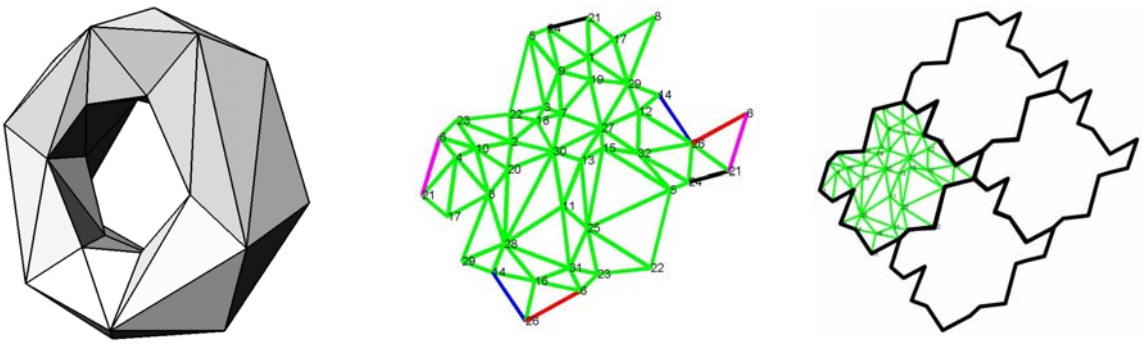

(a) (b) (c)

Figure 7: Parameterization of a torus containing 32 vertices and 64 faces. **(a)** 3D torus. **(b)** Parameterization of the torus to the plane using two harmonic one-forms generated with uniform weights. Vertices are numbered. The color coded edges along the boundary correspond. **(c)** Double periodic tiling of the plane using the drawing in (b).

Although we will not prove this, we believe that a toroidal mesh with boundaries ("holes") may be locally parameterized in an injective embedding in a manner similar to that of Section 3.2, namely, by allowing vertices along the boundaries to be non-harmonic, as long as they have turning number -2π, and the reflex vertices are wheels.

5. Higher Genus

While we have applied our Index Theorem (Theorem 2.5) only to the disk and to the genus 1 case to prove Tutte-like theorems, the theory is applicable also to higher genus meshes, except there matters are more complicated. By Theorem 4.1, the dimension of the space of harmonic one-forms for $g>1$ is at least

4 and so there are many fundamentally different “pairs of harmonic one forms” that can be chosen from the space in order to create a parameterization.

In addition, for $g>1$, the Index Theorem implies the existence of at least two saddle vertices and/or faces in every such harmonic one-form. So *something* must go awry when we apply the parameterization approach of Section 4.

As suggested by Gu and Yau [14], the “best” one can hope for is to have all of the "badness" in the parameterization isolated at $2g$-2 vertices or faces. In this case we may have a vertex that is *doubly wheel*, where the co-boundary edges will cycle in the drawing around the vertex twice. Or we may have a face that is *doubly convex*, where the boundary edges cycle around the face twice (see third column of figure 3). At these bad spots, the embedding cannot be even locally injective. Note that if the mesh has only triangular faces, only double-wheels may occur.

Here we prove that if a pair of harmonic one-forms is chosen such that it has $2g$-2 such *doubles,* then the rest of the resulting parameterization is locally injective.

Theorem 5.1: If G is a closed oriented 3-connected manifold mesh of genus g, and Δx and Δy are one-forms on G and $[G,x,y]$ - the corresponding drawing in the plane - contains $2g$-2 vertices or faces that are doubly wheel/convex, then all other vertices of $[G,x,y]$ are wheels and all faces are convex.

Proof: In *any* projection of $[G,x,y]$, a vertex that is doubly wheel, or face that is doubly convex, will be a saddle. If there are $2g$-2 doubles, then the Index Theorem (Theorem 2.5) implies that there can be no other saddles. So all other vertices and faces are always non-singular in every projection, hence all other vertices must be wheels and all faces convex. ♦

Of course, since the mapping is not everywhere locally injective, it is obviously not globally injective. But the drawing will at least contain faces which are all oriented consistently.

While we do not have a closed characterization of which two independent one-forms from the $2g$-dimensional solution space will, when used as x and y coordinates in the plane, form such an embedding, we can generate them using the following randomized (Las-Vegas) algorithm:

1. Compute a basis of the $2g$-dimensional solution space of the harmonic equations (1) and (2).
2. Select a one-form Δx at random from the space whose basis was computed in (1), e.g. a random linear combination of the basis functions. When integrated, this one-form will generate the x coordinate of the embedding.
3. Solve for another one-form Δy such that $[G,\Delta x,\Delta y]$ has $2g$-2 “doubles”. Since Δx has been fixed in step 2, this can be written as a linear program. In this program, every corner of the saddles of Δx is constrained to have a positive angle (i.e. positive cross product of the two one-forms at that corner). If it exists, this Δy is called a *mate* of Δx.
4. If step 3 failed, goto step 2.

It is easy to see that if Δx and Δy are mates, then any two linear combinations of Δx and Δy are also mates. Hence, in practice, it is possible to impose orthogonality of Δx and Δy in the linear program solved in Step 3.

We emphasize that Step 3 does indeed fail for some random choices made in Step 2, meaning there do exist one-forms Δx for which there is *no* mate Δy (not even the Δy generated by applying the discrete Hodge star operation [14] to Δx). However, in practice, the linear program fails to find a mate in Step 3

only rarely, so the algorithm usually terminates after a small number of steps. We have observed experimentally, though, that this failure rate increases with the genus.

The embeddings in Figure 8 were generated using this algorithm.

We conclude this discussion by stating some natural questions which are left open:

1. Which vertices in G can be saddles in a harmonic one-form? (We know that vertices with valence 3 cannot be saddles, because three edges cannot generate more than 2 sign changes of the one-form.)
2. Which vertices in G can appear as double wheels. (We known vertices with valence ≤ 4 cannot be saddles since each of the four angles must be $< \pi$, yet their sum must be 4π).
3. If a vertex can be a saddle or double wheel, how can we generate a one-form or pair of one-forms having this property ?
4. Is there any natural characterization of the one-forms that have mates?

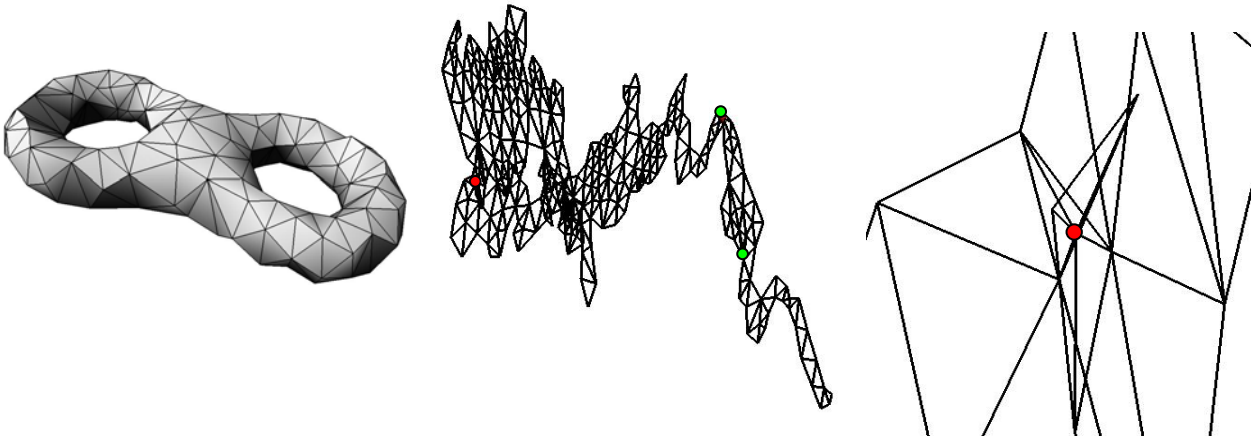

Figure 8: Parameterization of the two-hole torus. **Left:** the 3D mesh, containing 495 triangular faces. **Middle:** The parameterization of the mesh to the plane using uniform weights. The two double-wheel vertices are marked in red and green. The green one appears twice along the boundary. **Right:** Zoom into the red double-wheel vertex.

6. Conclusion

The concept of one-forms on meshes used in this paper, although simple, seems to be quite powerful. It unleashes a wealth of classical mathematical theory for which discrete analogs seem to exist. This is also related to some recent developments in polytopal graph theory [23] and planar tilings using harmonic functions on graphs [17].

This paper deals with the general case of asymmetric weights $w_{ij} \neq w_{ji}$ in (3). Many other papers (including Tutte [31]) deal only with the symmetric case. This is appealing because then the system has a physical interpretation of a spring system, and the Tutte solution minimizes the sum of the squares of the weighted spring lengths, hence the system's energy. Some of the recipes for generating barycentric coordinates for given embeddings yield symmetric weights, including the so-called cotangent weights [24]. However, most do not (e.g. the mean-value weights [9]), and it seems that the one-form theory presented here is powerful enough to deal with this.

Theorem 3.13 raises hope for other possible applications. One of these is constrained parameterization (see e.g. [18]), which is of paramount importance for texture mapping, guaranteeing that key features of a

texture are mapped to the corresponding features on a mesh. This problem calls to embed a disk-like mesh in the plane, such that the parameterization is injective, but also satisfies positional constraints at a (usually small) subset of the interior vertices. The results of Section 3 indicate that if all the "problematic" regions of the mesh are embedded properly, then harmonicity will take care of the rest. In the scenario of Section 3 – the problematic regions are the boundary vertices, which are taken care of either by forcing convexity or explicit wheels. This can be generalized to the case of constrained parametrization by considering the constrained vertices to also be "problematic" (or, in other words, part of a non-connected boundary), so it seems that forcing *both* the boundary vertices *and* the constrained vertices to be wheels should solve the problem. However, it remains to see how this can be done in a computationally efficient manner.

A possible application of local parameterization of the torus is for parameterizing a disk-like mesh with a free boundary. Since Tutte's theorem requires a convex boundary, one common way around this is to "pad" the disk with a number of layers of "virtual" faces, forming a new "virtual" boundary. This larger mesh is embedded in the plane using the convex boundary method, and the extra padding then discarded. This method, due to Lee et al [20], gives the true boundary more flexibility, and it will typically end up being non-convex. It is, however, still influenced by the virtual boundary and the connectivity of the virtual faces, hence is not artifact-free. Making use of our method for local parameterization of the torus, we believe it is more natural to embed the original disk within a *torus*, rather than a larger disk, as the torus seems to be the "cleanest" mesh. After solving for a harmonic one-form on the torus, this is transformed into an embedding of just the original disk-like submesh. This procedure eliminates boundary conditions entirely, hence should contain less artifacts.

References

[1] T.F. Banchoff. Critical points and curvature for embedded polyhedral surfaces. American Mathematical Monthly, 77:475-485, 1970.

[2] B. Becker and G. Hotz. *On the optimal layout of planar graphs with fixed boundary.* SIAM Journal of Computing, 16(5):946-972, 1987.

[3] I. Benjamini and L. Lovasz. *Determining the genus of a map by local observation of a simple random process.* Proceedings of the 43rd Annual Symposium on Foundations of Computer Science (FOCS), p. 701-710, 2002.

[4] H. Biermann, I. Martin, F. Bernardini and D. Zorin. *Cut-and-paste editing of multiresolution subdivision surfaces*. ACM Transactions on Graphics, 21(3):312-321, 2002 (Proceedings of SIGGRAPH).

[5] E. Colin de Verdière, M. Pocchiola and G. Vegter. *Tutte's barycenter method applied to isotopies.* Computational Geometry: Theory and Applications, 26(1):81-97, 2003.

[6] M. Desbrun, M. Meyer and P. Alliez. *Intrinsic parameterizations of surface meshes.* Computer Graphics Forum 21(2), 2002. (Proceedings of Eurographics).

[7] M.S. Floater. *Parameterization and smooth approximation of surface triangulations.* Computer Aided Geometric Design, 14:231–250, 1997.

[8] M.S. Floater. *One-to-one piecewise linear mappings over triangulations*. Mathematics of Computation, 72:685-696, 2003.

[9] M. S. Floater. *Mean value coordinates.* Computer Aided Geometric Design, 20:19-27, 2003.

[10] M.S. Floater and C. Gotsman. *How to morph tilings injectively*. Journal of Computational and Applied Mathematics, 101:117-129, 1999.

[11] M.S. Floater and K. Hormann. *Recent advances in surface parametrization.* Proceedings of the MINGLE workshop on Multiresolution in Geometric Modeling, Cambridge, Springer, 2003.

[12] M.S. Floater and V. Pham-Trong. *Convex combination maps over triangulations, tilings, and tetrahedral meshes*, To appear in Advances in Computational Mathematics, 2004.

[13] C. Gotsman and V. Surazhsky. *Guaranteed intersection-free polygon morphing.* Computers and Graphics, 25(1):67-75, 2001.

[14] X. Gu and S.-T. Yau. *Global conformal surface parameterization*. Proceedings of the ACM/Eurographics Symposium on Geometry Processing, Aachen 2003.

[15] N. Hirani. *Discrete Exterior Calculus.* Ph.D. Thesis, California Institute of Technology, 2000.

[16] T. Kanai, H. Suzuki and F. Kimura. *Metamorphosis of arbitrary triangular meshes.* IEEE Computer Graphics and Applications 20:62-75, 2002.

[17] R. Kenyon. *Tilings and discrete Dirichlet problems.* Israel Journal of Mathematics, 105:61-84, 1998.

[18] V. Kraevoi, A. Sheffer and C. Gotsman. *Matchmaker: Constructing constrained texture maps.* ACM Transactions on Graphics (Proceedings of SIGGRAPH 2003), 2003.

[19] F. Lazarus and A. Verroust. *Level set diagrams of polyhedral objects*. Proceedings of ACM Solid Modeling '99, June 1999.

[20] Y. Lee, H.S. Kim, and S. Lee. *Mesh parameterization with a virtual boundary.* Computers & Graphics, 26(5):677-686, 2002.

[21] N. Linial, L. Lovasz and A. Wigderson. *Rubber bands, convex embeddings and graph connectivity.* Combinatorica, 8(1):91-102, 1988.

[22] C. Mercat. *Discrete Riemann surfaces.* Communications of Mathematical Physics, 218(1):77-216, 2001.

[23] J. Mihalisin and V. Klee. *Convex and linear orientations of polytopal graphs.* Discrete and Computational Geometry, 24:421-435, 2000.

[24] U. Pinkall and K. Polthier. *Computing discrete minimal surfaces and their conjugates.* Experimental Mathematics, 2(1):15-36, 1993.

[25] K. Polthier and E. Preuss. *Identifying vector fields singularities using a discrete Hodge decomposition.* In Proceedings of Visualization and Mathematics III, Eds: H.C. Hege, K. Polthier, pp. 113-134, Springer 2003.

[26] J. Richter-Gebert. *Realization spaces of polytopes.* Lecture Notes in Math #1643, Springer, 1996.

[27] A. Sheffer and E. de Sturler. *Parameterization of faceted surfaces for meshing using angle based flattening*, Engineering with Computers*,* 17(3):326-337, 2001.

[28] D. Steiner and A. Fischer. *Planar parameterization for closed 2-manifold genus-1 meshes.* Proceedings of ACM Solid Modeling, Genova, 2004.

[29] C. Thomassen. *Tutte's spring theorem*. Journal of Graph Theory 45:272-280, 2004.

[30] Y. Tong, S. Lombeyda, A. Hirani and M. Desbrun. *Discrete multiscale vector field decomposition.* In Proceedings of SIGGRAPH 2003.

[31] W.T. Tutte. *How to draw a graph.* Proceedings of the London Mathematical Society, 13(3):743-768, 1963.

[32] R.S. Varga. *Matrix Iterative Analysis.* Springer, 2000.

Appendices

The Appendices provide some technical theorems which simplify the main results of this paper. The theorems will be formulated for the case of a mesh with a disk-like topology and convex boundary. With the appropriate modifications, these theorems carry over to the other cases (non-convex boundary, higher genus) as described.

Appendix A: Perturbing a non-valid one-form into a valid one-form

We will show how any one-form on a disk-like mesh obtained from a Tutte solution that contains vanishing values may be converted into a valid one-form without changing the signs of any of the non-zero values. The resulting one-from may have non co-closed vertices. But as mentioned in Section 3, the key to Lemma 3.2 is that all but two of the vertices have both negative and positive values of the one-form on its co-boundary. This is weaker than the co-closed property. More formally:

Definition A.1: A vertex (resp. face) is *mixed* in a one-form if has at least one positive and at least one negative value of the one-form on its co-boundary δv (resp. boundary ∂f). ♦

Definition A.2: A one-form is called *mixed* if all its vertices and faces are mixed. A one-form is called *almost mixed* if all its faces are mixed and all its vertices are mixed, with the exception of at most two vertices. ♦

The following key result follows as a special case of Theorem 2.2 of Linial et al. [21]:

Lemma A.3: If G is a 2-connected manifold mesh $<\mathcal{V},\mathcal{E},\mathcal{F}>$ and s and t any two distinct vertices of G, then there exists a *valid* one-form $[G,\Delta f]$, whose faces are all closed and whose vertices, (except for s, which is a source, and t, which is a sink), are all co-closed with respect to *some* set of positive edge weights w_{ij}. ♦

Clearly such a $[G,\Delta f]$ is *almost mixed*.

Lemma A.4: Let Δz be a one-form derived from a Tutte solution as in Section 3.1. It is possible to construct a valid almost mixed one-form $\Delta z'$ such that for every e with $\Delta z_e \neq 0$, $\text{sign}(\Delta z_e)=\text{sign}(\Delta z'_e)$.

Proof: Denote by f_e the outer face of the mesh. Tutte's method dictates that ∂f_e is embedded as a non-degenerate convex polygon, with no two vertices coincident. In the rotated drawing $[G,w,z]$ (where the rotation is determined by α and β), the boundary loop ∂f_e has vertices on its left side, and vertices on its right side. The left side has a top (and bottom) vertex, as does the right side. With respect to a generic choice of α and β, both sides share their top (and bottom) vertex with each other. With respect to some specific choice of α and β, the upper or lower edges may be horizontal and so the two sides may not share their top (or bottom) vertices. In addition, if the boundary is only weakly convex, for a specific choice of α and β, there may be additional "strictly top" and "strictly bottom" vertices that are strictly in between the left and right sides.

Pick any two vertices s and t on ∂f_e that are not strictly top or strictly bottom vertices. Apply Lemma A.3 to obtain a valid almost mixed Δf. Choose ε small enough such that adding $\varepsilon\Delta f$ to Δz will not to change

the signs of the non-zero values of Δz, but, on the other hand, validates Δz. See Fig. 9 for an illustration of this.

Any degenerate face in Δz is determined completely by Δf, hence is mixed in $\Delta z'$. Any non-degenerate face f is mixed in Δz, hence for sufficiently small ε remains so in $\Delta z'$. Hence all faces are mixed in $\Delta z'$.

The sign pattern of any degenerate vertex v in Δz is completely determined in $\Delta z'$ by Δf. Since s and t were explicitly chosen to be non-degenerate vertices, a degenerate v cannot be one of the chosen s or t. Hence v must be co-closed in Δf and thus mixed in $\Delta z'$.

Any mixed vertex in Δz, for sufficiently small ε, must remain so in $\Delta z'$.

The only non-degenerate, not mixed vertices possible in Δz are the extreme ones: the top-left (TL), bottom-left (BL), top-right (TR), bottom-right (BR), strictly top (ST), and strictly bottom (SB) vertices. We now show that there cannot be more than two of these.

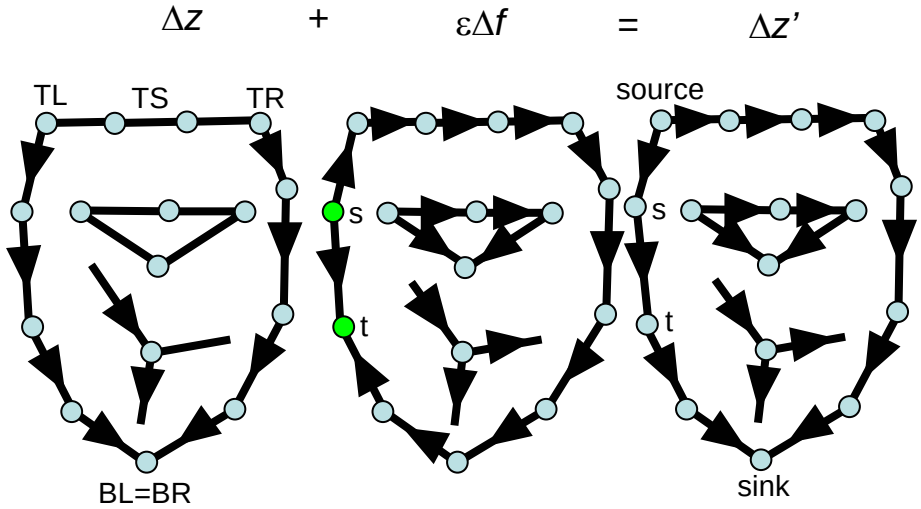

Figure 9: Scenario of Lemma A.4. Arrows mark the orientation of the half-edges possessing positive values of the one-form. Edges without arrows have invalid (zero) values.

If TL and TR coincide, then it can account for at most one non-mixed vertex in $\Delta z'$.

If TL and TR are distinct, then we use the following argument. By Lemma 3.2, there are no saddle faces in Δf, and so there can be only 2 sign changes as one circles ∂f_e (only at s and t). Hence $\Delta z'$ must go in one direction (wlog say from left to right) along the top (resp bottom) of ∂f_e. Therefore, the ST vertices and TR will have both positive and negative values on their co-boundaries in $\Delta z'$, hence be mixed. Thus TL can account for at most one non-mixed vertex.

An identical argument shows that BL and BR can account for at most one non-mixed vertex. ♦

The following lemma shows that if a vertex or face was a saddle in Δz, then it will certainly be a saddle in $\Delta z'$. Hence saddles cannot be eliminated by this perturbation of Δz. This is important for the proof of Theorem 3.6 to still hold after the perturbation.

Lemma A.5: If there were k sign changes around ∂f (δv resp.) in Δz, ignoring zeros, then index(f) $\leq 1-k/2$ (index(v) $\leq 1-k/2$ resp.) in Δz'.

Proof: The sign of a non-degenerate edge of Δz is preserved in $\Delta z'$. Hence the number of sign changes can only increase and the index only decrease. ♦

For the non-convex boundary, in Lemma A.4, we choose for s and t any two boundary vertices that have at least one boundary edge with non-zero value in Δz. The resulting perturbed one-form $\Delta z'$ will have the appropriate properties for Lemma 3.8 to apply.

For the torus, (and higher genus) case we must assume that the one-form is not completely degenerate. Then in Lemma A.4, we choose *any* two non-degenerate vertices to be s and t. The resulting perturbed one-form $\Delta z'$ will have *all* mixed vertices and faces and thus appropriate for Lemma 4.2 (resp. Theorem 5.1) to apply.

Appendix B: No degenerate vertices or faces

In this appendix we prove that a Tutte embedding does not contain degenerate elements. First we define what these are:

Definition B.1: Let Δz be a one-form on a mesh. A *degenerate* (half-)edge is one having vanishing value of the one-form. A *degenerate* face or vertex is one with all degenerate edges. A *degenerate* corner is one whose two edges are degenerate. ♦

For this Appendix we need a slightly stronger version of Lemma A.3, which also follows directly from a variant of the arguments in [21].

Lemma B.2: If G is a 2-connected manifold mesh $<\mathcal{V},\mathcal{E},\mathcal{F}>$, s and t any two distinct vertices of G, and p any directed simple path from s to t, then there exists a *valid* one-form [G,Δf], with all positive values along the half-edges of p, whose faces are all closed and whose vertices, (except for s, which is a source, and t, which is a sink), are all co-closed with respect to *some* set of positive edge weights w_{ij}. ♦

We now prove a series of lemmas leading to the desired result.

Lemma B.3: Let [G,x,y] be a Tutte solution. Then in any projected one-form [G,Δz] there can be no non-degenerate interior vertex participating in a degenerate corner.

Proof: Let v_0 be an interior vertex. Since it is non-degenerate, it must be mixed. We wish to show that if it participates in a degenerate corner, then we can find $\Delta z'$ - an appropriate perturbation of Δz of the form described in Lemma A.4 - which is a valid almost mixed one-form with a saddle at v_0. This would contradict Lemma 3.2.

Call the two edges of the degenerate corner e_{01}, e_{02}. These edges connect v_0 to v_1 and v_2. Since G is 3-connected, the graph G-$\{v_0\}$ is 2-connected. Therefore for any two vertices s and t we can find two vertex-disjoint paths connecting v_1 and v_2 to s and t (we cannot say in advance which will be connected to which) such that v_0 is not in either path [21]. By including all of the edges in these two paths in addition

to the edges e_{01} and e_{02}, we obtain a simple directed path from s to t that proceeds in the order $[v_1,v_0,v_2]$ or $[v_2,v_0,v_1]$. See Fig. 10. By Lemma B.2, there exists Δf: a valid almost mixed one-form with source s and sink t that either passes in order $[v_1,v_0,v_2]$ or $[v_2,v_0,v_1]$. Consider $\Delta z'=\Delta z+\varepsilon\Delta f$. This is a valid almost-mixed one-form with valid values on the edges e_{01} and e_{02}. With the proper choice of sign for ε, we can increases the number of sign changes around v_0, creating a saddle at v_0 in $\Delta z'$. This contradicts Lemma 3.2. ♦

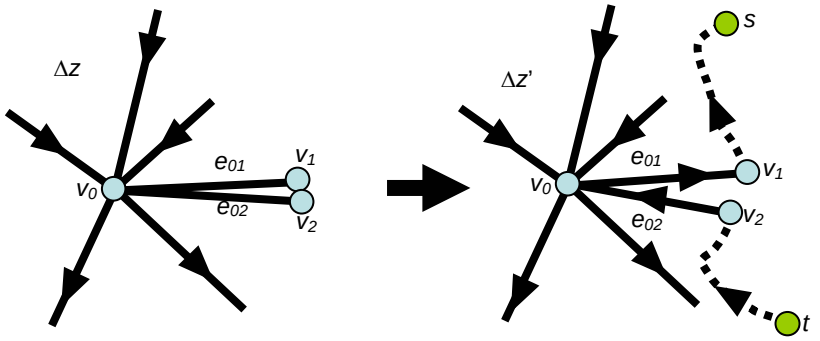

Figure 10: Scenario of Theorem B.3. Arrows mark the orientation of the half-edges possessing positive values of the one-form. Edges without arrows have invalid (zero) values.

Next we show that if there was any degenerate corner at an interior face, there would have to be some degenerate corner with a participating non-degenerate vertex.

Lemma B.4: Let $[G,x,y]$ be a Tutte solution. Then in any projected one-form $[G,\Delta z]$ there can be no degenerate corner at an interior face.

Proof: Assume (v_0,f) is a degenerate corner. If it is not part of a triangle (which would have to be degenerate by closedness), then introduce a new edge e_{12} between vertices v_1 and v_2 (the neighbors of v_0 at the degenerate corner); this splits f into a degenerate triangle and some remainder face. This *face-split* operation cannot change the 3-connectedness of G. The addition of this edge cannot change the co-closedness of v_1 and v_2. Repeat this operation for any degenerate corner. In the final G, any interior face with a degenerate corner must be a degenerate triangle.

Since $[G,x,y]$ is not degenerate, there must be some interior face f that is not degenerate sharing an edge e_{01}, between vertices v_0 and v_1, with a degenerate face. Either v_0 or v_1 must be an interior vertex, otherwise e_{01} would be an interior edge connecting two boundary vertices, which is impossible in a 3-connected planar graph.

WLOG, v_0 is an interior vertex. f has another vertex - v_3 - that shares an edge e_{03} with v_0. The one-form must be valid on this edge, otherwise e_{01} and e_{03} would have been a degenerate corner and f would have been a degenerate triangle. See Fig. 11. So v_0 is an interior non-degenerate vertex at a degenerate corner, in contradiction of Lemma B.3. ♦

Lemma B.5: In a Tutte solution there can be no face with zero area and no edge of zero length and no angle of 0 or π within any interior face.

Proof: Suppose there was a face with zero area. It is then possible to pick a projection (α,β) such that the resulting one-form vanishes on all edges of this face. Similarly, if there is an edge e with zero length, then pick (α,β) such that the resulting one-form will vanish on one of the edges neighboring on e. In both cases, we will have a degenerate corner in the one-form, in contradiction of Lemma B.4 ♦

The proofs of Appendix B apply directly to the non-convex boundary case of Theorem 3.13. They also apply directly to one-forms on the torus. The equivalent to Lemma B.4 for the torus will state that in *any* (not completely degenerate) harmonic one-form [G,Δ*z*], there can be no degenerate corner. This implies no geometric degeneraces in any drawing [G',*x*,*y*] integrated from a pair of non-degenerate harmonic one-forms.

Harmonic one-forms on higher genus meshes have saddle vertices or faces and are thus more complicated. In this case there will exist one-forms [G,Δ*z*] with degenerate corners. But, in the special cases treated by Theorem 5.1, the saddles are all "accounted for", so again, no degenerate corners can exist.

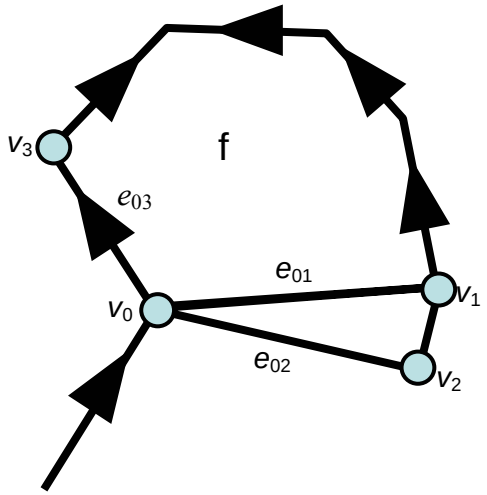

Figure 11: The scenario of Lemma B.4.